Available online at www.sciencedirect.com
SCIENCE DIRECT®
Journal of Molecular Catalysis A: Chemical 214 (2004) 293–300
JOURNAL OF MOLECULAR CATALYSIS A: CHEMICAL
www.elsevier.com/locate/molcata

Photocatalytic degradation of pesticide pyridaben in suspension of TiO_2: identification of intermediates and degradation pathways

Xinle Zhu [a,*], Xiaogang Feng [a], Chunwei Yuan [a,1], Xiaomei Cao [b], Jinheng Li [b]

[a] *The Laboratory of Nano-Materials and Photocatalysis, Southeast University, Nanjing 210096, PR China*
[b] *Department of Clinical Pharmacology, Jinling Hospital, Nanjing 210096, PR China*

Received 16 September 2003; received in revised form 3 January 2004; accepted 4 January 2004

Abstract

Photocatalytic degradation of pyridaben under UV irradiation has been investigated in acetonitrile/water solution containing TiO_2 particles. The primary degradation of the pollutant followed the Langmuir–Hinshelwood model with kinetic constant k, 4.3×10^{-5} mol/l min and equilibrium adsorption constant K, 3.1×10^{3} l/mol. Eight kinds of degradation products (DPs) were identified by GC–MS in the process of reaction and some of them were further confirmed by matching with authentic standards and synthesized compounds. Structure identification of DPs allowed us to propose the main degradation route. The key step was suggested to be the cleavage of C–S bond between phenyl ring and heterocyclic group. Meanwhile, frontier electron densities (FED) of pyridaben were theoretically studied on the basis of PM3 calculations for a better understanding of the reaction mechanism. The result indicated that the highest FED position was on the S atom of pyridaben molecule, where should be the starting point of the photocatalytic reaction, which is consistent with the experimental result.

Keywords: Pyridaben; Mechanisms; Photocatalysis; TiO_2; Frontier electron density (FED)

1. Introduction

Pyridaben (IUPAC name: 2-tert-butyl-5-[(4-tert-butylbenzyl)thio]-4-chloropyridazin-3(2H)-one), a new kind of insecticide, has been widely used in agriculture due to a very low animal toxicity, a juvenile hormone analog (JHA) and a broad spectrum pest control. It is applied for the control of spidermites (motile stages) and some insects (diptera, hemiptera, lepidoptera, thysanoptera especially toccidentalis) on ornamentals, pome fruit, stonefruit, citrus fruit, vegetables and alfalfa. Several studies have been devoted to toxicity tests as well as residue detect and management [1–3]. Since pyridaben is subjected to a mean persistence in the environment, there are relevant risks of leaching to surface water and in particular seeping into groundwater. Therefore, the investigation of viable remediation treatment of polluted waters from industrial effluents or agriculture runoff containing trace amounts of pyridaben is of environmental interest. In the past decades, heterogeneous photocatalysis [4–7] has been applied for water purification because of its efficiency in the mineralization of the aqueous pollutant in a short time. The present study deals with the photocatalytic degradation of pyridaben in the presence of TiO_2 particles and UV light. Pyridaben formula is given in Fig. 1. Three moieties characterize the molecule: a phenyl group, a C–S bridge, and a heterocyclic group. Photocatalytic degradation of nitrogen-containing heterocyclic compounds such as pyridine [8], pyrimidine [9–11], *S*-triazine [12,13] has been deeply investigated, however, to the best of our knowledge, there were few studies on the kind of pyridazine compounds [14]. In this paper, we report photocatalytic degradation of pyridaben for the first time. The objectives were to study the kinetics, solvent effect, and identify the main intermediates in order to determine the reaction mechanism, which was essential from an applicative point of view. Meanwhile, PM3 calculations were carried out in order to seek some essential correlations

* Corresponding author. Tel.: +86-25-8379-4310; fax: +86-25-8379-4310.
E-mail address: zhuxinle@seu.edu.cn (X. Zhu).
[1] Co-corresponding author.

1381-1169/$ – see front matter © 2004 Elsevier B.V. All rights reserved.
doi:10.1016/j.molcata.2004.01.001

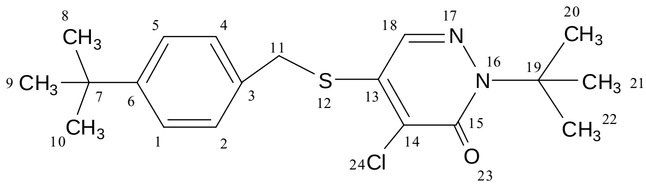

Fig. 1. Molecular structure of pyridaben.

between the simulated results and the experimental observations.

2. Experimental

2.1. Materials

P-25 TiO_2 was purchased from Degussa Co. The pesticide pyridaben and 2-tert-butyl-4,5-dichloropyridazin-3(2H)-one were kindly supplied by Jiangsu Red Sun Co. Ltd., and the former was re-crystallized to 99.92% in purity before use. Standards of the following compounds were used: 4-tert-butylphenyl-1-acetic acid and 1-tert-butyl-4-(chloromethyl) benzene from Nanjing University of Technology, 4-tert-butylphenol from Shanghai reagent Co., HPLC-grade acetonitrile and methanol were purchased from Tedia company Inc., water was Ultra-Pure water from Jiangsu Bote Purified Water Co. Ltd.

2.2. Light source and reactor

A 300 W medium-pressure mercury lamp was used as the light source. Light from this lamp was filtered through a circulating-water Pyrex glass cuvette to cut-off transmitting wavelengths $<$300 nm and to avoid heating of the solution. The photoreactor was placed at a fixed distance from the lamp housing (16 cm), where the radiant flux was equal to 10.1 mW/cm^2. A magnetic stirrer under the reactor was used to stir the solution.

2.3. Experimental setup and procedures

Pyridaben is nearly water-insoluble, so we examined the photocatalytic degradation via dissolution in acetonitrile/water (8/2) mixture. The aprotic acetonitrile was chosen as the solvent since it presented the best opportunity to control photocatalytic oxidative reactivity at the interface between a liquid reaction mixture and a solid irradiated photocatalyst. The suspension was left in the dark for 60 min to ensure establishment of adsorption equilibrium prior to illumination.

For the kinetic measurement, different initial concentrations of pyridaben were used to perform the photocatalytic reaction. Samples were taken at intervals, filtered with 0.22 μm millipore filter and applied to HPLC analysis. In order to characterize the intermediate products, the suspension of pyridaben with concentration of 7.02×10^{-4} mol/l was irradiated, filtered, distilled off the solvent by using a rotary evaporator under the reduced pressure, re-dissolved in dichloromethane and applied to GC–MS analysis. All the experiments were performed with 50 mg of powder TiO_2 (1 g/l) and the volume of 50 ml.

2.4. Analytical measurements

2.4.1. HPLC

Substrate conversions were monitored by high performance liquid chromatography (HPLC), using a 996 Photodiode Array Detector and Waters 510 pump. A good separation of the products was achieved using the reverse-phase column (Lischrospher, length 25 cm, inner 4.6 mm) and the detector with a wavelength at 296 nm, The mobile phase was composed of the following: 90% methanol, 10% water at pH 3 with H_3PO_4 buffer and at a flow rate of 0.7 ml/min.

2.4.2. GC–MS

To elucidate the structures of the intermediates, the concentrated sample solutions were subjected to GC–MS analysis. The GC (Agilent 6890 series) was equipped with a DB-5 capillary column (0.25 mm I.D., 0.32 μm film thickness, 30 cm length) and interfaced directly to the MS (micromass GCT) detector. The MS was operated with electron energy of 70 eV, an electron impact of ionization mode and a source temperature of 220 °C. The GC column was operated in a temperature programmed mode with an initial temperature of 110 °C held for 2 min and then ramped at 280 °C with a 10 °C/min rate. The concentrated solution was reconstituted with 100 μl of dichloromethane and 0.6 μl sample of this extract was injected in GC–MS in split mode (1:60) with helium as a carrier gas.

2.5. Synthesis of intermediates

Photodegradation product I reported in Fig. 2 was prepared by the method of Tomoyuki et al. [15] and intermediate II, 1-tert-butyl-4-ethylbenzene, was synthesized based on the procedure reported by Carpenter and Easter [16].

2.6. PM3 calculation

The optimal geometry conformation and the lowest energy of pyridaben molecule were obtained at PM3 level by choosing a charge of 0 and a spin of 1. By calculating the values of the FEDs of the highest occupied molecular orbitals (HOMO) through the summation of the square of wave function coefficient i.e. $f_k = \sum_j |C_{jk}|^2$, we derived the values of FED^2_{HOMO} to predict the reactive sites on pyridaben molecule for electron extraction by the photogenerated hole in the initial process. All calculations were carried out using Hyperchem, version 5.0.

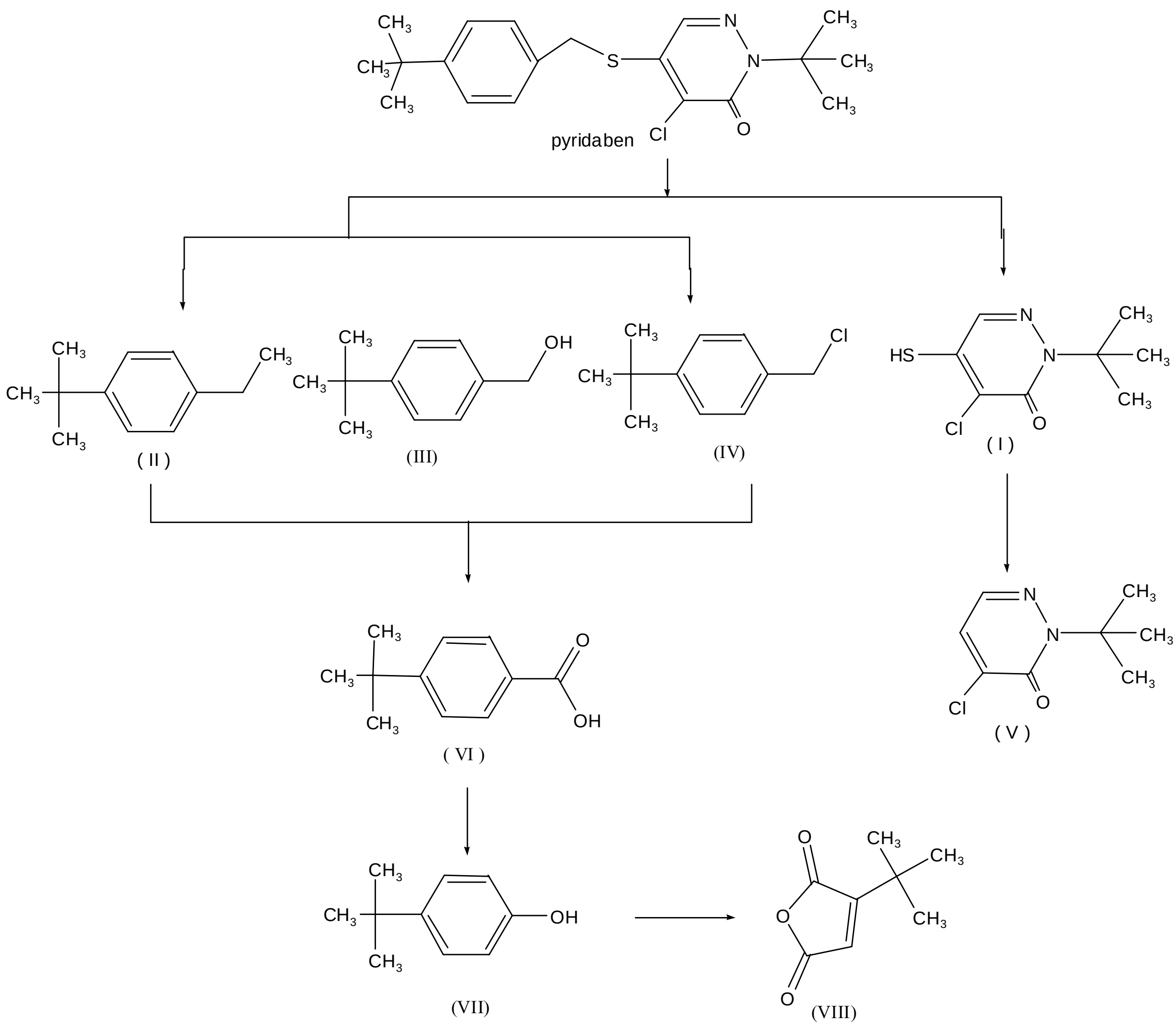

Fig. 2. Proposed degradation pathway of pyridaben.

3. Discussions

3.1. Kinetics of photocatalytic pyridaben

The kinetics of pyridaben degradation under the above conditions was stated by measuring the quantity of pyridaben remaining in the solution as a function of UV irradiation time. Fig. 3 shows the time courses of the photodegradation of pyridaben for different initial concentrations ranging from 1.5379×10^{-4} to 7.0257×10^{-4} mol/l with normalized concentrations C/C_0. From these plots, the initial rates of photocatalytic degradation pyridaben were obtained.

The decrease in the concentration of pyridaben could be accounted for by a Langmuir–Hinshelwood kinetic model:

$$r = k\theta = \frac{kKC}{1 + KC}, \quad (1)$$

where r is the oxidation rate of the reactant, θ the surface coverage, C the concentration of the reactant, k the rate constant, and K the equilibrium constant for the adsorption

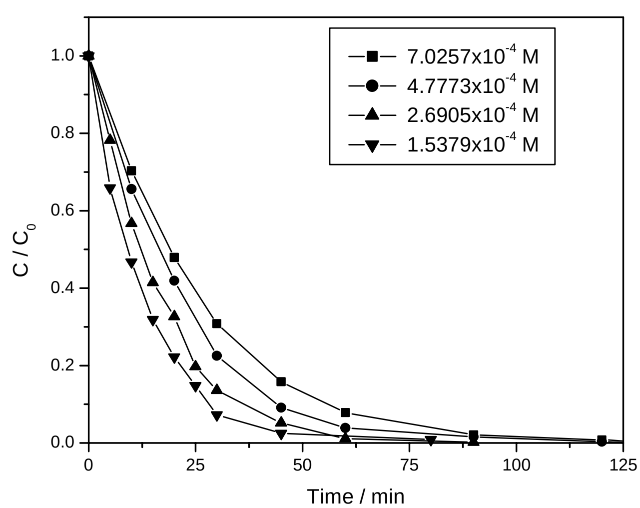

Fig. 3. Kinetics of pyridaben disappearance for various initial concentrations.

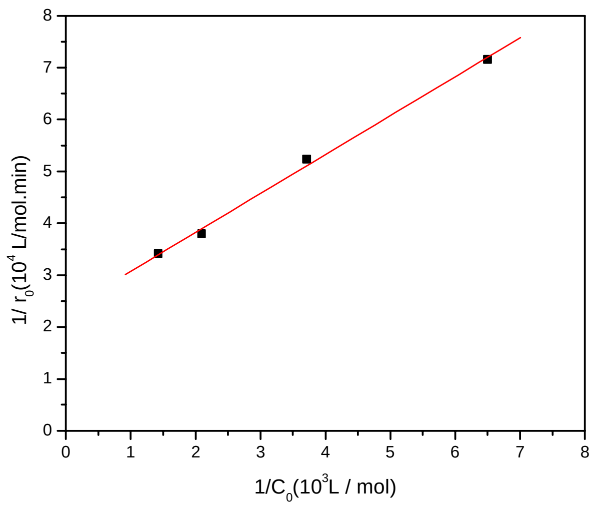

Fig. 4. Linear transform of reciprocal initial rates vs. reciprocal initial concentrations.

of the reactant. Inversion of this rate expression provides a linear plot:

$$\frac{1}{r} = \frac{1}{k} + \left(\frac{1}{kK}\right)\frac{1}{C} \tag{2}$$

In Fig. 4, the plot of reciprocal initial rates versus reciprocal initial pyridaben concentrations is presented, with which are obtained the slope $(kK)^{-1}$ and the intercept k^{-1}. So the values of the rate constant k, 4.3×10^{-5} mol/l min and equilibrium adsorption constant K, 3.1×10^{3} l/mol could be estimated, respectively, with correlation coefficient 0.9984.

The accurate amount of adsorption equilibrium in the dark was not worked out, because adsorbed pyridaben was minute within the limit errors of detection by HPLC. However, this limited adsorption did not prevent a rapid degradation, as described in Fig. 3. The apparent paradox phenomenon was reported by Marinas et al. [17] for the degradation of pesticide–acaricide formetanate and by Cunningham and Sedlack [18] for the degradation of benzylic alcohols and monochlorophenols. Mills and Hunte [19] also showed that the value of K derived from a kinetic study was not directly equivalent to the dark langmuir adsorption isotherm for substrate on the catalyst, the latter was usually smaller. Our experiments provided the further evidence.

The basic assumptions of the L–H kinetic model are that only one substrate may bind at each surface site and there is no interaction between adjacent adsorbed molecules [5]. While in the photocatalytic reaction, three possible situations exist [20]: (i) adsorbed photoactive oxygen interacts with the reactant adsorbed or in solution; (ii) hydroxy groups and water molecules cover a TiO_2 solid surface, they compete for the active sites of the catalyst; (iii) substrate photodecomposes giving rise to intermediates competitively on the surface of the catalyst. All these reflect in not ideal adsorption isotherms and mass transfer problems, so these reactions will require further study in detail. However, the above mentioned behavior is mainly to recombination reactions of active species but not adsorption properties of the substrate, the use of Langmuir–Hinshelwood equation could provide reasonable simulations to the observed degradation kinetics since the behavior of the reaction rate versus reactant concentration could be adjusted to a mathematical expression with it.

3.2. Identification of products

The solution of 87% of pyridaben removal was chosen to be analyzed by GC–MS. The gas chromatogram is presented in Fig. 5. Totally, up to eight intermediates were detected as degradation products of photocatalytic destruction of pyridaben. The molecular ion and spectrometric fragmentation peaks along with their relative intensities for the different products are given in Table 1. Products II, III, IV, V, VI, and VII were identified by comparing the MS spectra with corresponding products reported in the Nist and/or Willey library, with a similarity at least higher than 85% to the standard

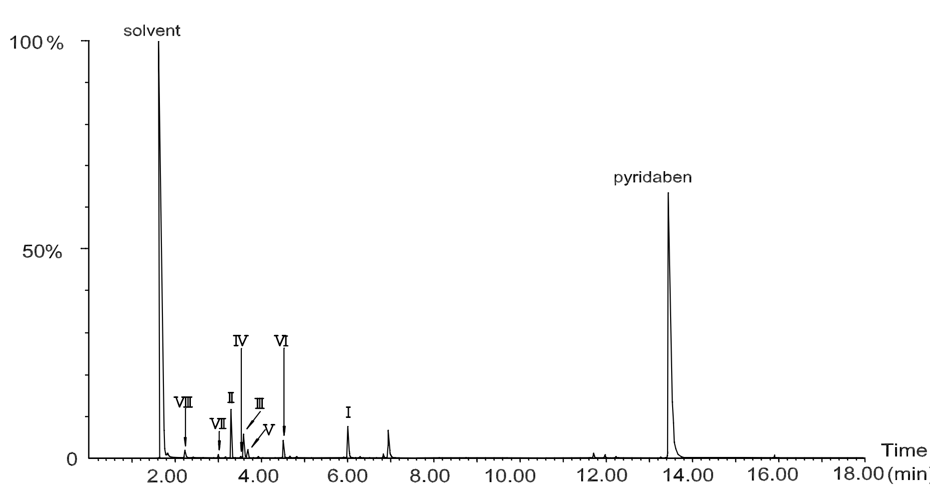

Fig. 5. Gas chromatograms of pyridaben and intermediates in photocatalysis.

Table 1
GC–MS-EI retention times (t_R) and spectra characteristics of pyridaben and its major photoproducts

Insecticide photoproducts	t_R (min)	EI-MS spectrum ions (*m/z*) (%, abundance)
Pyridaben	13.48	364(M^+)(5), 309(20), 311(4), 217(3), 147 (100), 132(5), 117(6), 55(6), 56(17), 57(3)
(I) 2-tert-Butyl-4-chloro-5-mercaptopyridazin-3(2H)-one	5.98	218(M^+)(18), 203(3), 165(30), 164(4), 163(100)162(12), 134(2), 105(2), 57(4), 56(8), 55(3)
(II) 1-tert-Butyl-4-ethyl benzene	3.28	162(M^+)(10), 147(100), 119(15), 115(3), 91(29)77(3), 51(2), 41(5)
(III) (4-tert-Butylphenyl) methanol	3.60	164(M+)(7), 149(100), 121(5), 119(10), 115(5), 91(29), 77(8), 51(8), 41(5)
(IV) 1-tert-Butyl-4-(chloro ethyl) benzene	3.53	182(M^+)(10), 184(3), 167(100), 169(25), 147(40), 139(27), 131(10), 91(48), 65(18)
(V) 2-tert-Butyl-4-chloropyridazin-3(2H)-one	3.70	186(M^+)(4), 133(25), 132(10), 131(100), 130(28), 73(11), 75(4), 57(25), 56(55), 55(18)
(V) 4-tert-Butylbenzoic acid	4.55	178(M^+)(8), 179(2), 163(100), 135(40), 115(3), 91(11), 77(2), 51(2), 41(5)
(VI) 4-tert-Butylphenol	3.08	150(M^+)(18), 135(100), 107(25), 95(17), 77(9), 40(20), 41(18)
(VII) 3-tert-Butylfuran-2,5-dione	2.25	139(M^+)(5), 126(65), 111(39), 95(62), 83(57), 67(100), 51(5), 419(10)

spectra. Compounds IV, V, and VI were further identified by matching their retention times and mass spectra with those of authentic standards.

Products I and II were characterized by comparison with synthesized compounds through GC–MS analysis under the same conditions. They exhibit the exact retention time and the similar mass spectra. The spectra are displayed in Figs. 6 and 7, respectively. On GC–MS a peak at $t_R = 3.70$ min shows the molecular ion $m/z = 186$, which is identified as intermediate V. Its mass spectrum and interpretation are shown in Figs. 8 and 9, respectively. A base fragment peak 131($M^+-C_4H_7$) appears with a typical isotope cluster *m/z* 133 of one Cl. In addition, fragments at *m/z* 130($M^+-C_4H_8$), 73($M^+-C_4H_7$–N_2–COH), 57($^+C_4H_9$), 56(C_4H_8) are presented, which exhibit the identical lose with compound I.

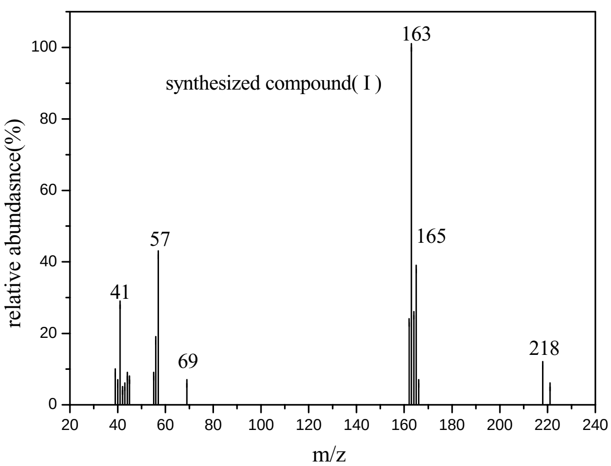

Fig. 6. Mass spectrum of the synthesized compound (I).

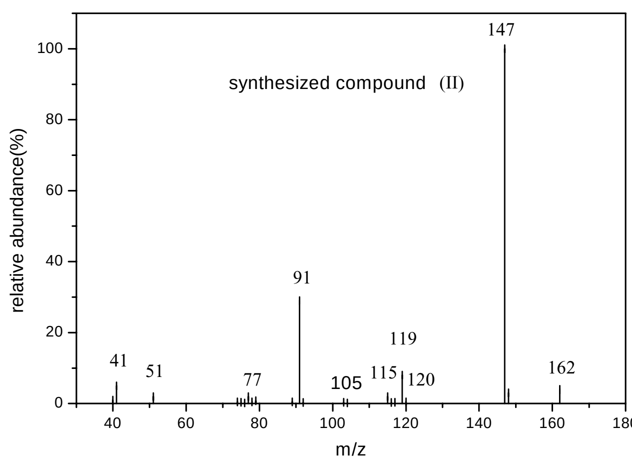

Fig. 7. Mass spectrum of the synthesized compound (II).

3.3. Proposal of degradation pathways

Taking into account the structure identification of eight intermediates and gas chromatograms derived at different irradiation time, we propose a reaction pathway for the

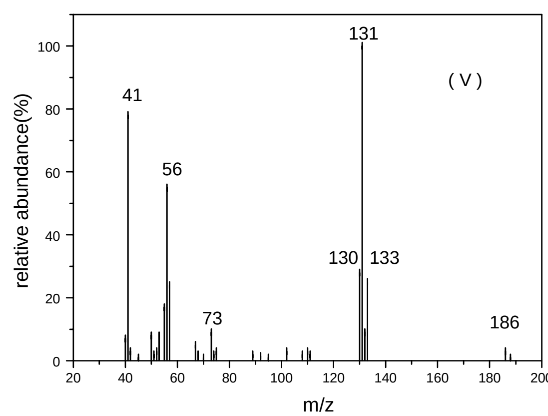

Fig. 8. Mass spectrum of compound (V).

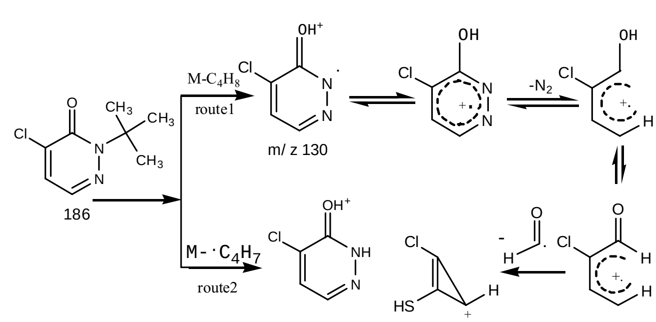

Fig. 9. MS interpretation of compound (V).

photocatalytic degradation of pyridaben, which is described in Fig. 2. The total degradation chart of TiO_2 photocatalysts of pyridaben could be understood briefly as following:

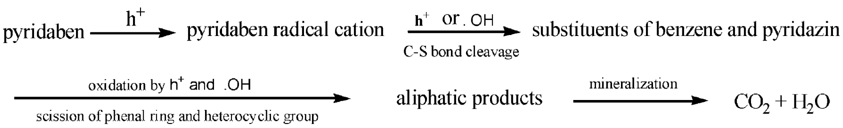

Irradiation of TiO_2 suspension with photons whose energy is equal to or higher than that of the band-gap energy of the semiconductor (e.g. 3.2 eV for TiO_2) causes conduction band electrons (e^-) and valance band holes (h^+). The photo-generated electrons (or holes) could reduce (or oxidize) organic substrates directly or react with the adsorbed molecular O_2 on the Ti(III) surface, reducing it to superoxide radical anion $O_2^{\bullet -}$. The photogenerated holes could also oxidize the OH^- ions and the H_2O molecules adsorbed on the TiO_2 surface to $^{\bullet}OH$ radicals. Together with other highly oxidant species they were reported to be responsible for the heterogeneous TiO_2 photodecomposition of organic substrates [4–6,21].

The initial photocatalytic degradation of pyridaben proceeds via C–S bond cleavage between phenyl ring and heterocyclic group. Firstly, oxidation of pyridaben molecule to form the pyridaben cation radical takes place by positive holes' attacking, and the mechanism has been proposed for the formation sulfide cation radicals. Fox and Abdel-Wahab [22,23] studied the TiO_2 mediated photocatalytic oxidation of benzyl and aryl sulfides, indicated that interfacial transfer of a single electron from the sulfur atom to form thioether cation radical, initiating C–S cleavage as a mechanism. More recently, Konstantinou et al. [24,25] also described the photocatalysis with TiO_2 of irgarol and molinate molecules generating an adsorbed sulfur cation radical by trapped a photogenerated hole and then the dealkylated product. Similar reaction was obtained by Abdel-Wahab et al. [26] that it was the photogenerated sulfur radical cations that initiated a series of reactions in photocatalytic oxidation of selected heterocyclic sulfur compounds. These considerations lead us to postulate the reaction mechanism of photocatalytic oxidation of pyridaben in the initial stage, i.e. direct oxidation of adsorbed substrate with photocatalyzed holes would form surface-bound cation radicals.

Fig. 10 describes two possible reaction pathways leading to the fission of C–S bond: (1) direct cleavage of C–S bond followed by the addition of H_2O molecules, methyl or chlorine radicals from the medium, result in the formation of compounds I, II, III, and IV; (2) pyridaben cation radical is extracted a proton to give pyridaben radical. This intermediate is further attacked by holes, and then reacts with H_2O molecules to yield the observed products I and III. Intermediates II, III, and IV could be further attacked on the aliphatic chain by $^{\bullet}OH$ radicals, strong electrophilic and oxidizing species, to form the corresponding alcohol, aldehyde and acid, i.e. $-CH_3 \rightarrow -CH_2OH \rightarrow -CHO \rightarrow -COOH$, subsequently, decarboxylate into CO_2 via the Photo-Kolbe reaction, $RCOO^- + h^+ \rightarrow R^{\bullet} + CO_2$. That the progressive

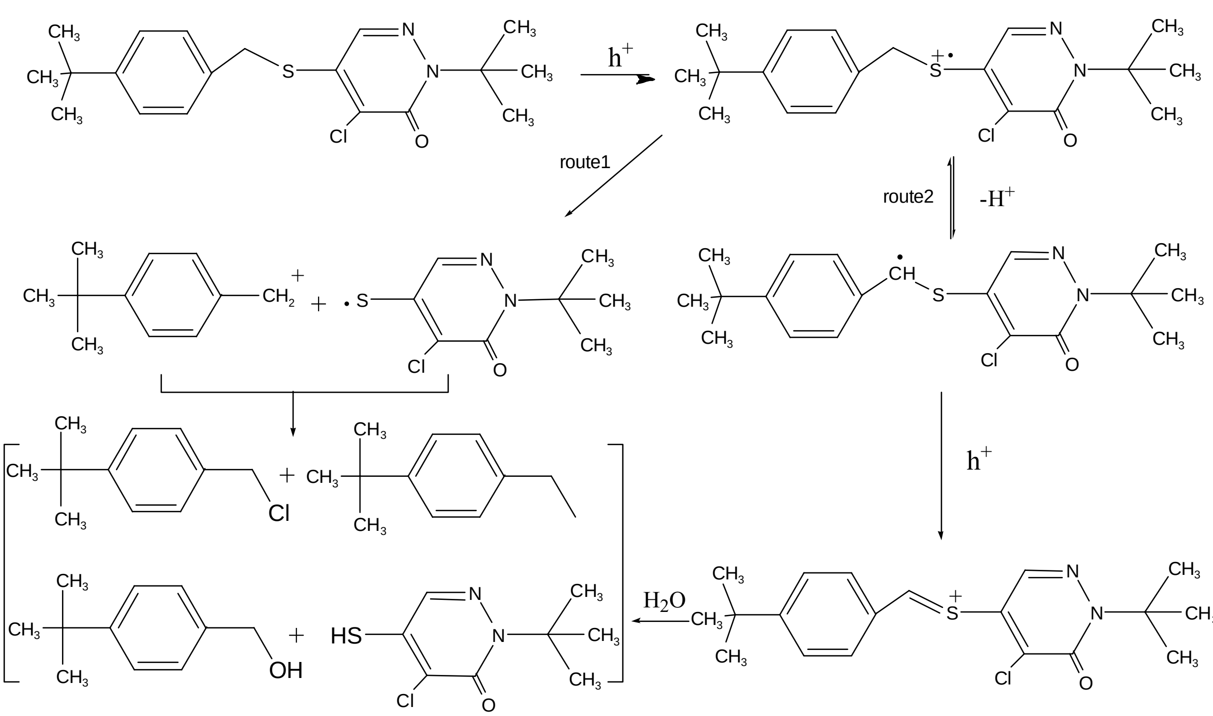

Fig. 10. Proposed photocatalytic mechanism for the C–S bond cleavage of pyridaben.

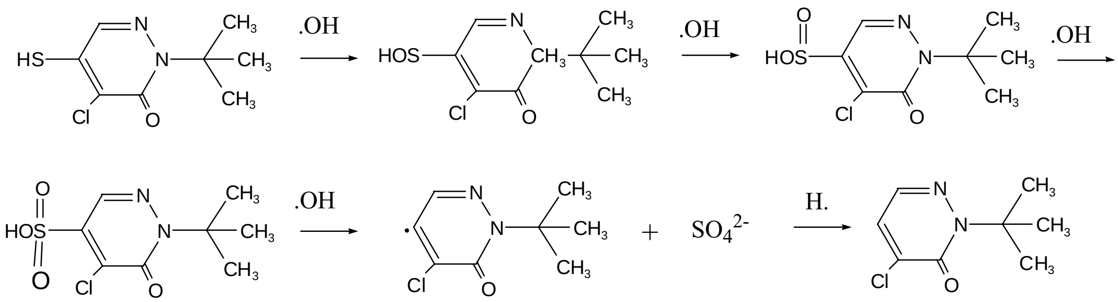

Fig. 11. Proposed reaction scheme for the formation of transformation product V.

degradation of side chains ascribed to the participation of hydroxyl radicals is previously observed [4,27]. Therefore, compound V is probably oxidized from II, III, and IV and then evolves to compound VI by Photo-Kolbe and •OH addition reactions, which is the last compound detected before the aromatic ring opening. Continuously attacking on the aromatic ring by •OH radicals leads to the ring opening and formation of aliphatic intermediate (VII), which is perhaps due to the dehydration of (2z)-2-tert-butylbut-2-enedioic acid. The further evolution to short chain acids and finally to CO_2, water, and other mineral compounds has been reported [4,28], so the formation of such intermediates is not investigated in the present study which mainly focuses on the major intermediates.

Oxidation of heterocyclic compound I is considered to be turned into compound V. The mechanism could be explained by the four-step reaction of S oxidation according to Fig. 11. Oxidation of sulfur atom of I by •OH radicals generates the sulfenic acid, sulfinic acid, and sulfonic acid successively. Final removing of $–SO_4{}^{2-}$ group from sulfonic acid forms $C_8H_{10}N_2OCl$ radical due to the fourth attack by •OH radical [5,19,29], and consecutive reaction with an H• radical produces compound V. Houas et al. [30] obtained a similar result in the study of photocatalytic degradation of methylene blue in water. The origin of H atoms necessary to S–H bond formation was proposed from the proton reduction by photogenerated electrons $H^+ + e^- \rightarrow H^\bullet$ as already observed in the degradation of insecticide fenitrothn by Mikhail et al. [31].

The compound IV is likely to form by adding a chlorine radical to 1-tert-butyl-4-methylbenzene radical, and Cl• radicals are originated by fission from heterocycle. 1-tert-Butyl-4-(chloroethyl) benzene is unstable in water [32], and further substitution by hydroxyl ion removes chloride ion to yield III rapidly. This consequence is analogous to that proposed previously for the heterogeneous photocatalysis of the 1,2-dichloroethane [33,34]. De-chlorination is a relatively rapid process, as the amount of IV indicates increasing and then disappearing in a more rapid time as shown in GCs.

3.4. Theoretical study

The mechanism of pyridaben degradation by TiO_2 photocatalysis is studied not only experimentally but also theoretically by calculating the frontier electron densities (FED). The frontier electron theory on the electrophilic reaction suggests that the position bearing higher FED on the highest molecular orbital (HOMO) in the ground state be more susceptible to be attacked [35]. In addition, by means of linear combinations of the orbitals [36], we approximate the one-electron wave functions, $\Psi_j = \sum_k C_{jk}\varphi_k$, where Ψ belongs to the different atoms, φ_k the $2p\pi$-atomic orbital of the kth atom, C_{jk} the value of the coefficient corresponding to the jth eigenvalue. Consequently, the density of each electron occupying the jth electronic level at the kth atom could be represented by $|C_{jk}|^2$, and the total average FED on atom k will be where the summation is extended over all occupied orbitals, i.e. $f_k = \sum_j |C_{jk}|^2$ [37]. The evaluated results are listed in Table 2. According to FED theory [38–41], we conclude that the primary position of pyridaben that loses an electron and is attacked by oxidant species would be those atoms with the largest frontier electron density, so the distribution of the FED^2_{HOMO} in pyridaben molecule will determine the degradation path in the initial photocatalytic stage. The results in Table 2 show that the largest FED^2_{HOMO} value is distributed at S atom where the electron would be most readily extracted to form pyridaben cation radical in TiO_2 photocatalysis, and then be continuously attacked by holes or •OH radicals. Therefore, the S atom in the pyridaben structure is proved to be a most reactive site with holes, which is consistent with the experimental results.

Table 2
Frontier electron densities (FED^2_{HOMO}) on atoms of pyridaben molecular at the PM3 level

Atoms	FED^2_{HOMO}	Atoms	FED^2_{HOMO}
C^1	0.00219	C^{13}	0.1533
C^2	0.00499	C^{14}	0.3953
C^3	0.0248	C^{15}	0.01257
C^4	0.00979	N^{16}	0.09567
C^5	0.00169	N^{17}	0.08949
C^6	0.00975	C^{18}	0.05552
C^7	0.00017	C^{19}	0.00069
C^8	0.00047	C^{20}	0.00015
C^9	0.00014	C^{21}	0.00267
C^{10}	0.00010	C^{22}	0.00280
C^{11}	0.01066	O^{23}	0.1546
S^{12}	0.5691	Cl^{24}	0.4115

4. Conclusions

In summary, we confirm the following in the present work:

(1) The primary degradation of pyridaben in acetnitrile/water follows the Langmuir–Hinshelwood model with kinetic constant k, 4.3×10^{-5} mol/l min and equilibrium adsorption constant K, 3.1×10^{3} l/mol.
(2) Eight kinds of intermediates are identified by GC–MS analysis, by comparison with authentic samples and synthesized compounds as well.
(3) The degradation pathway of pyridaben is proposed. It is suggested that the initial photocatalytic degradation proceeds mainly via C–S bond cleavage between phenyl ring and heterocyclic group. The C–S moiety of pyridaben molecule, one of the essential functional groups to interact with the oxidation species, especially the atom S should be the starting point of the photocatalytic oxidation. The formation of pyridaben radical cation is contributed to the initial reaction in the photocatalytic degradation. There exists a plausible consistent between experimental results and theoretical calculation on the basis of results obtained in present work.

Further studies on determination of the nature of unidentified products and the kinetic research of various intermediates are in progress and will be reported in the near future. The mechanism study of photocatalytic degradation is fundamentally necessary for a subsequent extension to large photocatalytic facilities.

Acknowledgements

This work is financially supported by Hi-Tech Research and Development Program (863 Program) of China (No. 2002AA302304). The authors are grateful to Prof. Yizu Wu of Nanjing University of Technology for providing standard TPs and directing the work on synthesis. We also wish to acknowledge helpful discussion with Prof. Degang Fu and Prof. Hong Zhang.

References

[1] J.L. Bi, N.C. Toscano, G.R. Ballmer, Crop Prot. 21 (2002) 49.
[2] P. Cabras, A. Angiono, V.L. Garau, M. Melis, F.M. Pirisi, F. Cabitza, F. Dedoia, S. Navickiene, J. Agric. Food Chem. 46 (1998) 4255.
[3] O. Hajime, S. Aakamoto, J. Pesticide Sci. 19 (1994) 243.
[4] R. Hoffmann, S.T. Martin, W. Choi, D.W. Behnemann, Chem. Rev. 95 (1995) 69.
[5] M.A. Fox, M.T. Dulay, Chem. Rev. 93 (1993) 341.
[6] O. Legrini, E. Oliveros, A.M. Braun, Chem. Rev. 93 (1993) 671.
[7] D.F. Ollis, E. Pelizzetti, N. Serpone, Environ. Sci. Technol. 25 (1991) 1523.
[8] G.K.-C. Low, S.R. Mcevoy, R.W. Mattews, Environ. Sci. Technol. 25 (1991) 460.
[9] S. Horikoshi, N. Serpone, S. Yoshizawa, J. Knowland, H. Hidaka, J. Photochem. Photobiol., A 120 (1999) 63.
[10] J.-M. Herrmann, C. Guillard, M. Arguello, A. Aguera, A. Tejedor, L. Piedra, A. Fernandez-Alba, Appl. Catal., B 54 (1999) 353.
[11] C. Jaussaud, O. Paisse, R. Faure, J. Photochem. Photobiol., A 130 (2000) 157.
[12] E. Vulliet, C. Emmelin, J-M. Chovelon, C. Guillard, J.-M. Herrmann, Appl. Catal., B 38 (2000) 127.
[13] E. Pellzzettl, V. Maurino, C. Mlnero, V. Carlin, E. Pramauro, O. Zerblnatl, M.L. Tosato, Environ. Sci. Technol. 24 (1990) 1559.
[14] S. Horikoshi, H. Hidaka, J. Photochem. Photobiol., A 141 (2001) 201.
[15] O. Tomoyuki, K. Yasuo, S. Hideos, Pyrazolecarboxylates, JP P, 61109777.
[16] M.S. Carpenter, W.M. Easter, J. Org. Chem. 19 (1954) 87.
[17] A. Marinas, C. Guillard, J.M. Marinas, A.F. Alba, A. Aguëra, J.-M. Herrmann, Appl. Catal., B 34 (2001) 241.
[18] J. Cunningham, P. Sedlack, in: D.F. Ollis, H. Al-Ekabi (Eds.), Photocalytic Purification and Treatment of Water and Air, Elsevier, Amsterdam, 1993, p. 67.
[19] A. Mills, S.L. Hunte, J. Photochem. Photobiol., A 108 (1997) 1.
[20] P. Fernández-Ibáñez, S. Malato, F.J. de las Nieves, Catal. Today 54 (1999) 195.
[21] I.K. Konstantinou, T.M. Sakellarides, V.A. Sakkas, T.A. Albanis, Environ. Sci. Technol. 35 (2001) 398.
[22] M.A. Fox, A.A. Abdel-Wahab, Tetrahedron Lett. 31 (1990) 4533.
[23] M.A. Fox, A.A. Abdel-Wahab, J. Catal. 126 (1990) 693.
[24] I.K. Konstantinou, T.M. Sakellarides, V.A. Sakkas, T.A. Albanis, Environ. Sci. Technol. 35 (2001) 398.
[25] I.K. Konstantinou, V.A. Sakkas, T.A. Albanis, Appl. Catal., B 34 (2000) 227.
[26] A.-M. Abdel-Wahab, A.E.-A.M. Gaber, J. Photochem. Photobiol., A 114 (1998) 213.
[27] T. Sakata, T. Kawai, K. Hashimoto, J. Phys. Chem. 88 (1984) 2344.
[28] A. Assabane, Y.A. Ichou, H. Tahiri, C. Guillard, J-M. Herrmann, Appl. Catal., B 24 (2000) 71.
[29] G. Mascolo, A. Lopez, R. Foldenyi, R. Passino, G. Tiravanti, Environ. Sci. Technol. 29 (1995) 2987.
[30] A. Houas, H. Lachheb, M. Klaloui, C. Guillard, J.-M. Herrmann, Appl. Catal., B 31 (2001) 145.
[31] K. Mikhail, C. Guillard, J.-M. Herrmann, P. Pierre, Catal. Today 27 (1996) 215.
[32] A.M. Perio, J.A. Ayllon, J. Peral, X. Domenech, Appl. Catal., B 30 (2001) 359.
[33] J.-C. D'Ollveira, G. A-Sayyed, P. Pichat, Environ. Sci. Technol. 24 (1990) 990.
[34] D.F. Ollis, C.-Y. Hsiao, L. Budiman, C.-L. Lee, J. Catal. 88 (1984) 89.
[35] K. Fukui, T. Yonezawa, C. Nagata, H. Shingu, J. Chem. Phys. 22 (1954) 1433.
[36] G.W. Wheland, et al., J. Am. Chem. Soc. 57 (1935) 2086.
[37] K. Fukui, T. Yonezawa, H. Shingu, J. Chem. Phys. 20 (1952) 722.
[38] Y. Ohki, K.-I. Iuchi, C. Niwa, T. Tatsuma, T. Nakashima, T. Iguchi, Y. Kubota, A. Fujishima, Environ. Sci. Technol. 36 (2002) 4175.
[39] K. Fukui, T. Yonezawa, C. Nagata, H. Shingu, J. Chem. Phys. 22 (1954) 1433.
[40] S. Horikoshi, N. Serpone, J. Zhao, Hidaka, H. Hidaka, J. Photochem. Photobiol., A 118 (1998) 123.
[41] G. Liu, X. Li, J. Zhao, S. Horikoshi, H. Hidaka, J. Mol. Catal., A 153 (2000) 221.